


Article

# Liquid Chromatography Tandem Mass Spectrometry Quantification of $^{13}\text{C}$ -Labeling in Sugars

Jean-Christophe Cocuron <sup>1</sup>, Zacchary Ross <sup>2</sup> and Ana P. Alonso <sup>1,3,\*</sup> <sup>1</sup> BioDiscovery Institute, University of North Texas, Denton, TX 76203, USA; Jeanchristophe.Cocuron@unt.edu<sup>2</sup> Heritage College of Osteopathic Medicine, Ohio University, Dublin, OH 43016, USA; zross913@gmail.com<sup>3</sup> Department of Biological Sciences, University of North Texas, Denton, TX 76203, USA

\* Correspondence: Anapaula.Alonso@unt.edu; Tel.: +1-940-369-5229

Received: 20 December 2019; Accepted: 8 January 2020; Published: 10 January 2020



**Abstract:** Subcellular compartmentation has been challenging in plant  $^{13}\text{C}$ -metabolic flux analysis. Indeed, plant cells are highly compartmented: they contain vacuoles and plastids in addition to the regular organelles found in other eukaryotes. The distinction of reactions between compartments is possible when metabolites are synthesized in a particular compartment or by a unique pathway. Sucrose is an example of such a metabolite: it is specifically produced in the cytosol from glucose 6-phosphate (G6P) and fructose 6-phosphate (F6P). Therefore, determining the  $^{13}\text{C}$ -labeling in the fructosyl and glucosyl moieties of sucrose directly informs about the labeling of cytosolic F6P and G6P, respectively. To date, the most commonly used method to monitor sucrose labeling is by nuclear magnetic resonance, which requires substantial amounts of biological sample. This study describes a new methodology that accurately measures the labeling in free sugars using liquid chromatography tandem mass spectrometry (LC-MS/MS). For this purpose, maize embryos were pulsed with [U- $^{13}\text{C}$ ]-fructose, intracellular sugars were extracted, and their time-course labeling was analyzed by LC-MS/MS. Additionally, extracts were enzymatically treated with hexokinase to remove the soluble hexoses, and then invertase to cleave sucrose into fructose and glucose. Finally, the labeling in the glucosyl and fructosyl moieties of sucrose was determined by LC-MS/MS.

**Keywords:** sucrose; glucose 6-phosphate; fructose 6-phosphate; subcellular compartmentation;  $^{13}\text{C}$ -labeling; LC-MS/MS; hexokinase; invertase;  $^{13}\text{C}$ -metabolic flux analysis

## 1. Introduction

Metabolic flux is the flow of matter through a metabolic step or pathway. The goal of  $^{13}\text{C}$ -metabolic flux analysis (MFA) is to quantify all the *in vivo* intracellular metabolic fluxes in a given organ or cell, which results in a metabolic flux map. While only a few fluxes, such as the rates of substrate uptake and product accumulation can be measured directly, determination of intermediary carbon fluxes requires  $^{13}\text{C}$ -labeling. Labeled plant tissues/cells are usually harvested after they have reached isotopic steady-state, meaning that the labeling in intermediary metabolites and products have reached a constant pattern. The resultant labeling in a range of metabolites is then determined using nuclear magnetic resonance (NMR), which gives positional isotopomers information, while mass spectrometry (MS) is used to provide mass isotopomer information [1].

First MFA studies considered cells as a unique compartment where organelles were not taken into account [2–4]. Although the importance of subcellular compartmentation in the regulation of metabolism is well established [5,6], its application in MFA—especially in plants—has been challenging. Indeed, plant cells are highly compartmented: in addition to the regular organelles found in other eukaryotes, they contain vacuoles and plastids. Consequently, different pools of the same metabolite can be present in different compartments, and some reactions and even entire pathways are duplicated,

which adds to the complexity of applying MFA to plant cells [1,7]. For instance, glucose 6-phosphate (G6P), one of the intermediaries of the glycolysis, is commonly found in the cytosol where it serves as a precursor for sucrose and cell wall biosynthesis, and in the plastid where it is involved in starch production. Similarly, the full glycolytic pathway is usually redundant between the cytosol and the plastid. Recent ion chromatography tandem mass spectrometry techniques have been developed to directly monitor the labeling of various glycolytic intermediaries, such as G6P [8,9]. However, the metabolite extraction procedure is pooling together compounds present in different organelles, which results in an average labeling for each intermediary and hence a loss of subcellular information.

The distinction of reactions between compartments is possible when metabolites are synthesized in a particular compartment or by a unique pathway [10]. For instance, starch is exclusively produced in the plastid, and its labeling pattern is a direct reading of the labeling in plastidic hexose-phosphates (Figure 1). Sucrose is another example of such a metabolite: it is specifically synthesized in the cytosol from G6P and fructose 6-phosphate (F6P) through the activity of the sucrose phosphate synthase (#10, Figure 1). Therefore, determining the  $^{13}\text{C}$ -labeling in the fructosyl and glucosyl moieties of sucrose directly informs about the labeling of cytosolic F6P and G6P, respectively. The capability of distinguishing between the hexose-phosphates from the cytosol and the plastid has been crucial to determine: (i) the subcellular location of the oxidative pentose phosphate pathway; (ii) the exchange rates of hexose-phosphates between these two compartments; and (iii) the portion of the glycolytic flux occurring in the cytosol vs. the plastid (Figure 1) [11–19]. Additionally, the analysis of the labeling of the free sugars also lead to the discovery of a cytosolic cycle re-synthesizing glucose from G6P through the synthesis and degradation of sucrose and/or the activity of a potential glucose 6-phosphatase [11–17,19,20]. Substrate cycles are also called “futile cycles” because they consume ATP without apparent physiological function [21]. Indeed, these processes can be high-energy demanding and the overall ATP consumption varies from 5% to 70%, depending on the plant organ [2,12,13,17,19,20].

Although a recent study used high-resolution mass spectrometry to determine the labeling of free sugars (glucose, fructose, and sucrose) in plant cells, it does not provide information on the glucosyl and fructosyl units from sucrose [22]. To date, the most commonly used method to monitor the labeling in sucrose fructosyl and glucosyl moieties is by NMR [11–19,23]. Although NMR provides positional labeling information, its sensitivity is limited in comparison to MS, consequently requiring substantial amounts of biological sample. This study describes a new methodology that accurately measures the labeling in free sugars using liquid chromatography tandem mass spectrometry (LC-MS/MS) in multiple reaction monitoring mode. This approach was applied to monitor the time-course labeling of glucose, fructose, sucrose and its glucosyl and fructosyl moieties in maize embryos incubated with [U- $^{13}\text{C}$ ]-fructose.

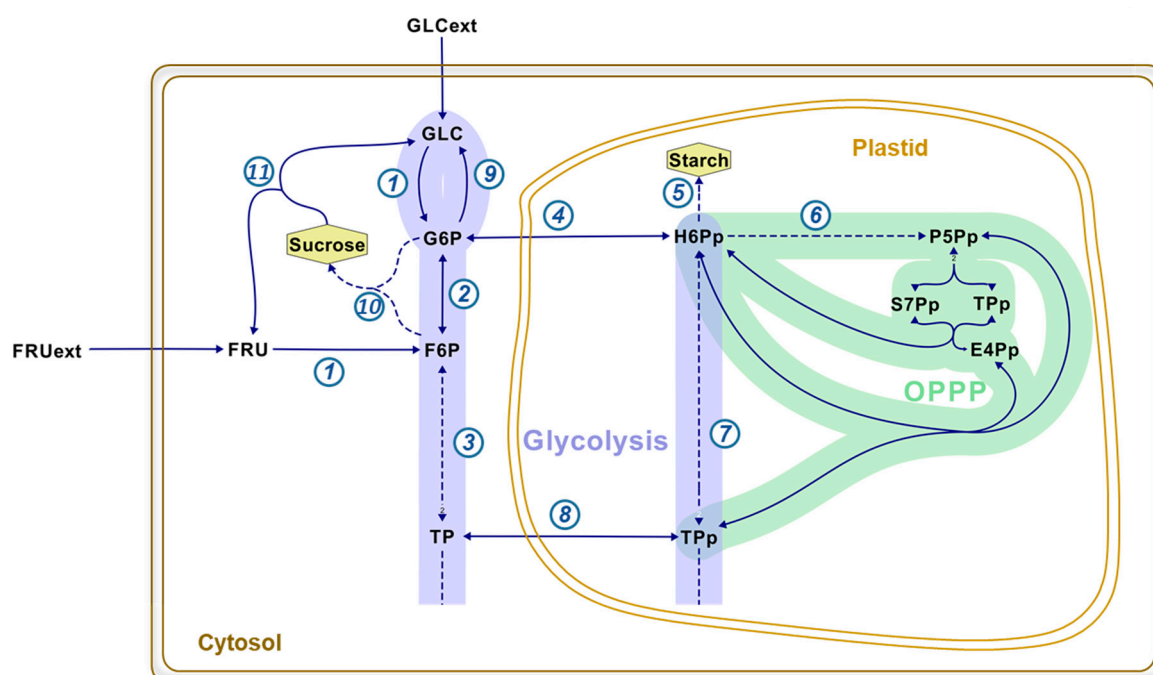


**Figure 1.** Representative example of maize embryos to illustrate the subcellular compartmentation of hexose-phosphates in plant cells. Developing maize embryos mainly import glucose and fructose as carbon sources. These sugars get phosphorylated into hexose-phosphate in the cytosol. The resulting hexose-phosphates are involved in major pathways: glycolysis (purple), and the oxidative pentose-phosphate pathway (OPPP; green). Full and dashed arrows represent one reaction or a multiple-step reaction, respectively: 1 is hexokinase; 2, phosphoglucose isomerase; 3 and 7, cytosolic and plastidial aldolases, respectively; 4 and 8, exchange of hexose-phosphates and triose-phosphates between cytosol and plastid, respectively; 5, starch synthesis; 6, oxidative part of the OPPP; 9, glucose 6-phosphatase; 10, sucrose phosphate synthase; and 11, invertase. Abbreviations in alphabetical order: E4Pp, plastidic erythrose 4-phosphate; FRU(ext), (extracellular) fructose; F6P, fructose 6-phosphate; GLC(ext), (extracellular) glucose; G6P, glucose 6-phosphate; H6Pp, plastidic hexose-phosphates; P5Pp, plastidic pentose-phosphates; S7Pp, plastidic sedoheptulose 7-phosphate; TP(p), (plastidic) triose-phosphates.

## 2. Results and Discussion

### 2.1. LC-MS/MS Analysis of Free Sugars

Maize ears were harvested at 18 days after pollination (DAP), and embryos were dissected from the kernels, lyophilized and ground into a fine powder. Free sugars were extracted using boiling water, and analyzed by LC-MS/MS as previously described [16,24]. Briefly, sugars were separated using a gradient of acetonitrile and water on a Shodex Asahipak NH2P-50 2D column (2.0 × 150 mm) and a Shodex Asahipak NH2P-50G 2A guard column. The detection was performed by a triple-quadrupole QTRAP 5500 from AB Sciex in negative mode using multiple reaction monitoring (MRM) and parameters listed in Table 1. Hexoses and disaccharides were followed using transitions 179/89 and 341/59, respectively, which correspond to [parent]/[daughter] ion formulas of  $[C_6H_{11}O_6^-]/[C_3H_6O_3^-]$  and  $[C_{12}H_{21}O_{11}^-]/[C_2H_4O_2^-]$  [25]. This methodology was demonstrated to successfully separate sugar isomers: (i) fructose, mannose, galactose, glucose, and inositol, and (ii) sucrose, maltose, and trehalose [24].

**Table 1.** Mass spectrometry parameters for the detection of sugars. DP: Declustering potential, EP: Entrance potential, CE: Collision energy, CXP: Collision cell exit potential, are described for hexoses and disaccharides. Parent and daughter ion formulas were reported by Calvano et al. [25].

Sugars	Parent Ion Formula	Daughter Ion Formula	Parent/Daughter Transitions	DP (V)	EP (V)	CE (V)	CXP (V)
Hexoses	$C_6H_{11}O_6^-$	$C_3H_6O_3^-$	179/89	-30	-10	-12	-11
Disaccharides	$C_{12}H_{21}O_{11}^-$	$C_2H_4O_2^-$	341/59	-240	-10	-50	-9

Three main sugars were found in maize embryos: (i) fructose was followed in the transition of the hexoses (179/89) with a retention time of 5.11 min; (ii) glucose, another hexose (transition 179/89), comes at 7.90 min; and (iii) sucrose was monitored in the transition of the disaccharides (341/59) and has a retention time of 11.95 min (Figure 2A).

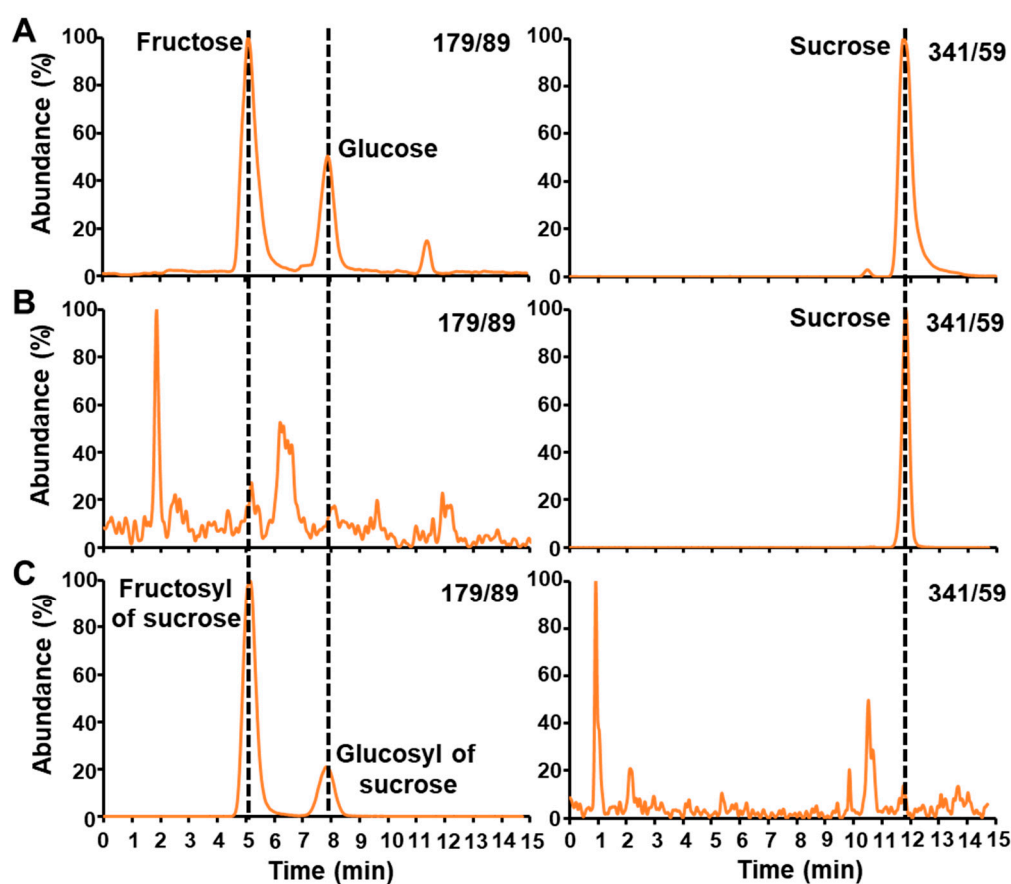


**Figure 2.** LC-MS/MS chromatograms of free sugars before and after enzymatic treatments. (A) shows the chromatographic separation and mass spectrometric detection of fructose, glucose (transition 179/89), and sucrose (transition 341/59) after boiling water extraction of unlabeled maize embryos. (B) and (C) represent the LC-MS/MS chromatograms obtained after hexokinase and invertase treatments, respectively. LC-MS/MS chromatograms for hexoses and sucrose were obtained using MRM scan survey approach as indicated in the Materials and Methods.

## 2.2. LC-MS/MS Analysis of the Glucosyl and Fructosyl Moieties of Sucrose

Boiling water extractions from maize embryos were treated first with a hexokinase from *Saccharomyces cerevisiae* for two hours in order to phosphorylate the free glucose and fructose into G6P and F6P, respectively. As shown in Figure 2B, the hexokinase entirely converts all the hexoses present in maize embryos. Indeed, no peaks of glucose and fructose were detected at their expected retention

time after this operation. It is important to note that the sucrose was left intact (Figure 2B). Then, an invertase from *Saccharomyces cerevisiae* was added for two hours in order to cleave the sucrose into its fructosyl and glucosyl moieties. The resultant sugars units were analyzed by LC-MS/MS (Figure 2C). Invertase cleaved all the sucrose, which is denoted by the absence of a peak at its expected retention time. The fact that no sucrose was detected after invertase treatment indicates that it was entirely converted into glucose and fructose. Indeed, two peaks appears in the transition of the hexoses (179/89) corresponding to the fructosyl and glucosyl of sucrose.

Sucrose is an important metabolite in terms of subcellular localization: it is specifically synthesized in the cytosol from G6P and F6P by the activity of the sucrose phosphate synthase (#10, Figure 1). The enzymatic steps described above will give access to the  $^{13}\text{C}$ -labeling in the fructosyl and glucosyl moieties of sucrose, which will directly inform about the labeling of cytosolic F6P and G6P, respectively.

### 2.3. Application of LC-MS/MS to Monitor $^{13}\text{C}$ -Labeling in Free Sugars

Previous labeling experiments consisted in incubating maize embryos from 15 to 21 DAP with  $^{13}\text{C}$ -labeled glucose until isotopic steady state, and revealed the occurrence of cycle of re-synthesis of glucose from G6P [11,16]. However, steady state labeling does not allow the distinction between the sucrose substrate cycle and the glucose 6-phosphatase activity because both reactions result in the same labeling distribution. To discern between the two potential reactions, a pulse labeling experiments is required. For this purpose, maize embryos were harvested at 18 DAP (corresponding to the half-time of the previous steady state labeling experiments), and pulsed with  $[\text{U-}^{13}\text{C}]$  fructose for 1, 2, 5, 20, 80, 320, 1280, 2730, 4160, and 5600 min while the other carbon sources in the medium were  $^{12}\text{C}$ -glucose and  $^{12}\text{C}$ -glutamine. We strategically chose to use  $[\text{U-}^{13}\text{C}]$  fructose, and to monitor the appearance of the labeling in free intracellular glucose as an additional proof that these substrate cycles are occurring in plant cells. Intracellular sugars were extracted from labeled maize embryos using boiling water. The time-course labeling of free glucose, fructose, and sucrose was monitored by LC-MS/MS using multiple reaction monitoring mode and MS parameters listed in Tables 1 and 2.

**Table 2.**  $^{13}\text{C}$ -labeled sugar isotopomers using MRM. RT: Retention time.

Sugars	RT (min)	Mass Isotopomers	Parent/Daughter Transitions
Fructose	5.11	m <sub>0</sub>	179/89
Glucose	7.90	m <sub>1</sub>	180/89; 180/90
		m <sub>2</sub>	181/89; 181/90; 181/91
		m <sub>3</sub>	182/90; 182/91; 182/92
		m <sub>4</sub>	183/90; 183/91; 183/92
		m <sub>5</sub>	184/91; 184/92
		m <sub>6</sub>	185/92
		Sucrose	11.95
m <sub>1</sub>	342/59; 342/60		
m <sub>2</sub>	343/59; 343/60; 343/61		
m <sub>3</sub>	344/59; 344/60; 344/61		
m <sub>4</sub>	345/59; 345/60; 345/61		
m <sub>5</sub>	346/59; 346/60; 346/61		
m <sub>6</sub>	347/59; 347/60; 347/61		
m <sub>7</sub>	348/59; 348/60; 348/61		
m <sub>8</sub>	349/59; 349/60; 349/61		
m <sub>9</sub>	350/59; 350/60; 350/61		
m <sub>10</sub>	351/59; 351/60; 351/61		
m <sub>11</sub>	352/60; 352/61		
m <sub>12</sub>	353/61		

The  $^{13}\text{C}$ -isotopomer abundances of fructose and glucose are reported in Table S1. Figure 3 depicts the relative abundances of the isotopomers m<sub>0</sub> (unlabeled hexose), m<sub>3</sub> (labeled in three carbons),

and  $m_6$  (fully labeled) over the entire time course, and the first 80 min. The uptake of  $[U-^{13}C]$ -fructose from the medium is quickly labeling the intracellular fructose whose  $m_0$  rapidly decreased to 16.7% within the first 5 min, and then slowly reached a value of 4.9% at 5600 min. On the other hand, the fully labeled fructose ( $m_6$ ) reached 76.7% the first 5 min of the pulse, and continued to steadily increase to 83.4% at the end of the incubation. Interestingly, the appearance of other mass isotopomers, such as  $m_3$ , was also monitored and will be discussed below (Figure 3, Table S1 (Supplementary Materials)). The labeling profile was found to be much slower for intracellular glucose due to the uptake of unlabeled glucose from the medium. Indeed, the occurrence of  $m_3$  and  $m_6$  only started after 320 min of incubation and their relative abundance reached 5.9% and 8.5%, respectively (Figure 3, Table S1 (Supplementary Materials)).

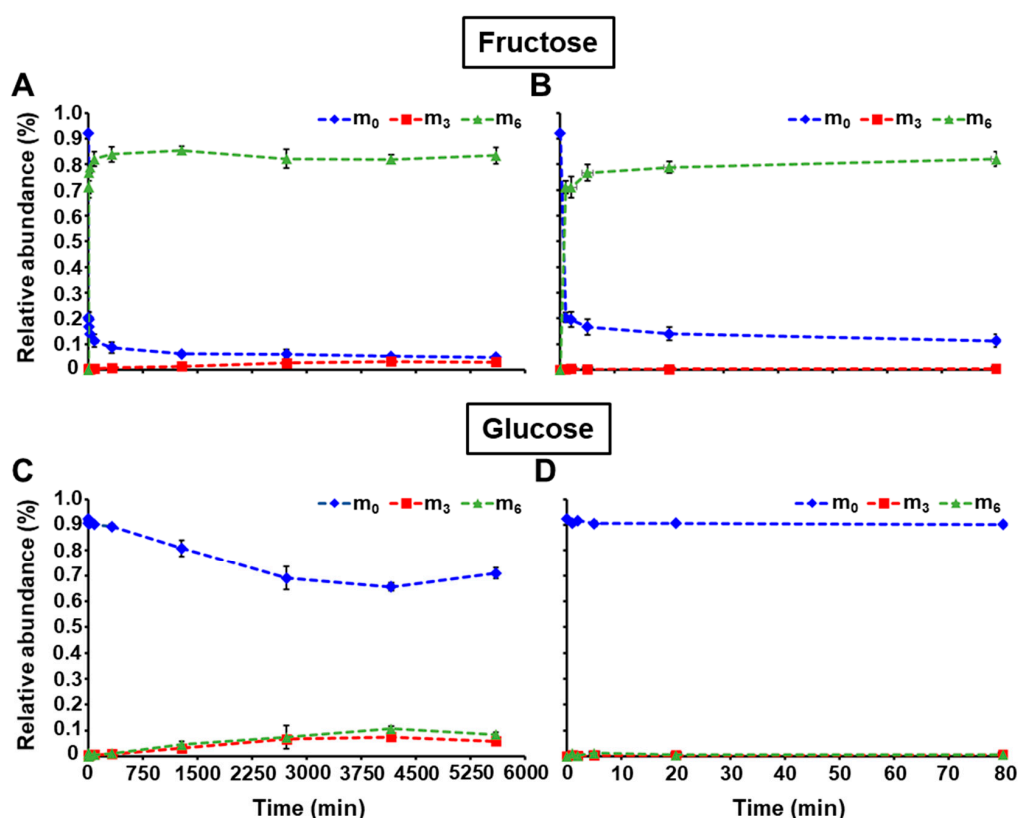


**Figure 3.** Relative abundance of isotopomers for intracellular fructose and glucose during pulse labeling with  $[U-^{13}C]$ fructose. (A,C) show the relative abundance of mass isotopomers at all time points for fructose and glucose, respectively. (B,D) represent the relative abundance of mass isotopomers from 0 to 80 min for fructose and glucose, respectively. Intracellular glucose and fructose were extracted, and analyzed as described in the “Materials and Methods” section. Mass relative abundances (in %) were reported as the average  $\pm$  SD ( $n = 4$  biological replicates). Mass isotopomers  $m_0$ ,  $m_3$ , and  $m_6$  are depicted as blue diamond, red square, and green triangle, respectively.

The relative abundance of intracellular sucrose mass isotopomers is detailed in Table S2 (Supplementary Materials), and plotted in Figure 4A,B. Additionally, maize embryo extracts were enzymatically treated with hexokinase to remove the soluble hexoses, and then invertase to cleave sucrose into fructose and glucose. Finally, the labeling in the glucosyl and fructosyl moieties of sucrose were monitored by LC-MS/MS using the same parameters reported in Table 2, and the relative abundance of their mass isotopomers was determined (Table S2 (Supplementary Materials), Figure 4). The abundance of unlabeled intracellular sucrose ( $m_0$ ) quickly decreased to 15.7% in 1280 min, and then stabilized to approximately 10% towards the end of the incubation (Figure 4A,B). This profile is due to a fast appearance of  $m_6$  which reached 41.7% within 1280 min, and then plateaued at around 32%.



In parallel, sucrose  $m_{12}$ ,  $m_9$ , and  $m_3$  increased up to 14.0%, 10.3%, and 5.3%, respectively over the time course. The relative abundances of the unlabeled fructosyl and glucosyl moieties decreased at different rates (Figure 4C–F). Fructosyl  $m_0$  quickly dropped to 15.8% in 1280 min, whereas the abundance of glucosyl  $m_0$  was still at 55.2% at this time point and continued to slowly decline to 37.8% at 5600 min. For the  $m_6$  of sucrose fructosyl, the abundance rapidly culminated at 73.6% within 1280 min, and then diminished to 59.2% due to the appearance of other mass isotopomers, such as  $m_3$  that went up to 9.0% by the end of incubation. Fully labeled glucosyl moiety of sucrose constantly increased over the time course to reach 25.6% of abundance while the  $m_3$  plateaued to 12.3% after 2720 min.

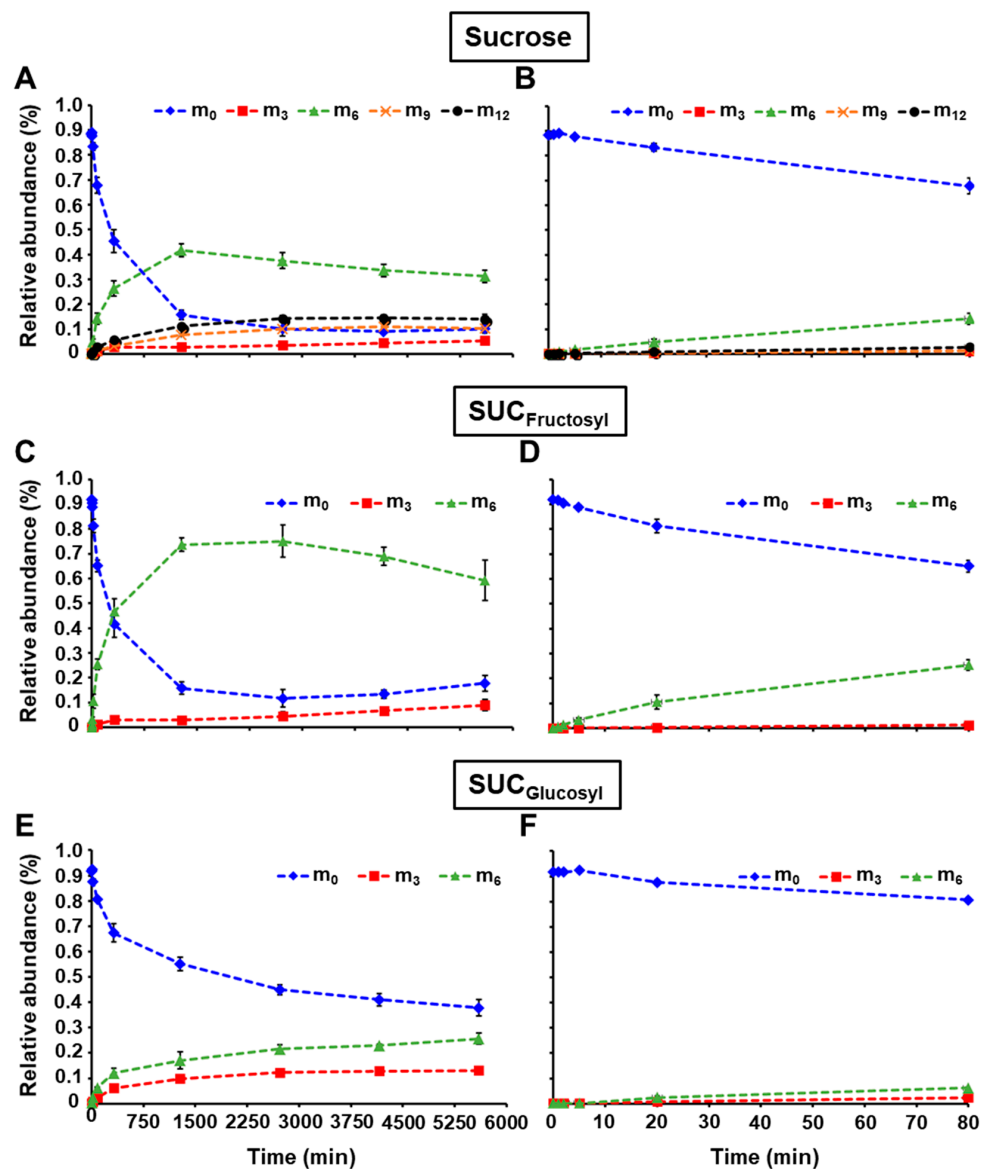


**Figure 4.** Relative abundance of isotopomers for  $^{13}\text{C}$ -fructosyl and  $^{13}\text{C}$ -glucosyl units from sucrose during the pulse labeling experiment. (A,C,E) represent the relative abundance of mass isotopomers at all time points for sucrose,  $\text{SUC}_{\text{Fructosyl}}$ , and  $\text{SUC}_{\text{Glucosyl}}$ , respectively. (B,D,F) depict the relative abundance of mass isotopomers from 0 to 80 min for sucrose,  $\text{SUC}_{\text{Fructosyl}}$ , and  $\text{SUC}_{\text{Glucosyl}}$ , respectively. Sucrose was extracted, cleaved into its fructosyl and glucosyl units, and analyzed as described in the Materials and Methods section. Mass relative abundances (in %) were reported as the average  $\pm$  SD ( $n = 4$  biological replicates). Mass isotopomers  $m_0$ ,  $m_3$ ,  $m_6$ ,  $m_9$ ,  $m_{12}$  are shown as blue diamond, red square, green triangle, orange cross, and black circle, respectively.  $\text{SUC}_{\text{Fructosyl}}$ : Sucrose fructosyl;  $\text{SUC}_{\text{Glucosyl}}$ : Sucrose glucosyl.

With the methodology described here, the  $^{13}\text{C}$ -labeling was successfully determined in the fructosyl and glucosyl moieties of sucrose, which directly informs about the labeling of cytosolic F6P and G6P, respectively (Figure 1). The occurrence of  $m_3$  in sucrose fructosyl (F6P) is due to the reversibility of the aldolase, which combines two triose-phosphates into one hexose-phosphate (#3, Figure 1). Similarly, the appearance of  $m_3$  and  $m_6$  in sucrose glucosyl (G6P) reflects the activity of the phosphoglucose isomerase (#2, Figure 1). The fact that  $m_3$  increased in intracellular fructose demonstrates that a sucrose cycle of synthesis and degradation is occurring in developing maize embryos (#10 and 11, Figure 1). It is noteworthy to mention that there is no fructose 6-phosphatase indexed in MetaCyc nor KEGG Ligand database, so the only way to obtain fructose with three labeled carbons is through this sucrose substrate cycle. This is in accordance with previous  $^{13}\text{C}$ -metabolic flux analysis studies performed at isotopic and metabolic steady state [11,12,15–17,19]. Knowing that in the present work, maize embryos were fed with  $[\text{U-}^{13}\text{C}]$ fructose and unlabeled glucose, the reactions to explain the incidence of labeling in intracellular glucose ( $m_3$  and  $m_6$ ) are by sucrose substrate cycle (#10 and 11, Figure 1) and/or a potential glucose 6-phosphatase activity (#9, Figure 1). The sucrose substrate cycle produces intracellular glucose and fructose at the same rate. However, the glucose  $m_3$  appeared 2.4 times faster than the fructose  $m_3$  (Figure 3A,C). This phenomenon underlines that both sucrose substrate cycle and glucose 6-phosphatase activity are simultaneously occurring in developing maize embryos. These results corroborate previous studies in maize root tips [13,14,20].

### 3. Materials and Methods

#### 3.1. Chemicals

Glucose, fructose, glutamine, polyethylene glycol 4000 (PEG), 4-(2-Hydroxyethyl)piperazine-1-ethanesulfonic acid (HEPES), hexokinase (from *Saccharomyces cerevisiae*), invertase (from *Saccharomyces cerevisiae*), were purchased from Sigma (St. Louis, MO, USA).  $[\text{U-}^{13}\text{C}]$  fructose was purchased from Isotec (Miamisburg, OH, USA). Acetonitrile, and methanol LC-MS grade were ordered from Fisher Scientific (Hampton, NH, USA).

#### 3.2. Plant Materials and Growth Conditions

Maize (*Zea Mays* L.) seeds for ALEXHO S K SYNTHETIC C20 (Alex, NSL 117227) were obtained from the U.S. National Plant Germplasm System. Maize Alex plants were grown in a greenhouse, hand pollinated, and ears were harvested as previously described [16]. For cultures, 18 DAP maize ears were surface sterilized [26]. Briefly, after removing the inner husks and silks, maize ears were taken to a laminar flow bench. Each ear was sterilized for 20 min in 50% bleach (*v/v*), and then rinsed and soaked for 20 min in autoclaved water. Maize embryos were dissected under aseptic conditions, and transferred into the incubation media previously described [16,26]: glucose (200 mM), fructose (200 mM), glutamine (5 mM), MS basal salts (4.3 g/L), 15% polyethylene glycol 4000, MES buffer (10 mM), and a mixture of vitamins containing nicotinic acid (5  $\mu\text{g}/\text{mL}$ ), pyridoxine hydrochloride (0.5  $\mu\text{g}/\text{mL}$ ), thiamine hydrochloride (0.5  $\mu\text{g}/\text{mL}$ ), and folic acid (0.5  $\mu\text{g}/\text{mL}$ ). The pH was adjusted to 5.8 with 1N potassium hydroxide. Maize embryos were placed scutellum up in glass petri dishes, on double-glass fiber filters soaked with 8 mL of the medium described above. Petri dishes were sealed with surgical tape. For pulse labeling experiments, fructose was replaced by 100%  $[\text{U-}^{13}\text{C}]$  fructose whereas glucose and glutamine remained unlabeled. Maize embryos were incubated in plates for 0, 1, 2, 5, 20, 80, 320, 1280, 2730, 4160, and 5600 min in the dark at 24 °C. One embryo was harvested for each time point as previously described [11]. Briefly, each embryo was collected and rinsed three times with 10 mL of water to remove surface labeling. The embryo was then frozen with liquid nitrogen and lyophilized for four days. Each pulse labeling experiment was conducted with four biological replicates.



### 3.3. Extraction of Soluble Sugars

Free soluble sugars were extracted from ground freeze-dried maize embryos using boiling water, and following an established procedure [9,24,26,27]. It is important to note that no  $^{13}\text{C}$ -labeled internal standards were added at the time of extraction. The extracts containing free sugars were freeze-dried, and stored at  $-20\text{ }^{\circ}\text{C}$  until further analysis.

### 3.4. Analysis of $^{13}\text{C}$ -Labeling in Free Sugars

An amount of 300  $\mu\text{L}$  of ultra-pure water was added to the dried extract containing  $^{13}\text{C}$ -free intracellular sugars (fructose, glucose, and sucrose).  $^{13}\text{C}$ -sucrose was hydrolyzed into its  $^{13}\text{C}$ -fructosyl and  $^{13}\text{C}$ -glucosyl units, which are reflecting the labeling of cytosolic F6P and G6P, respectively. First, 100  $\mu\text{L}$  of the free sugar sample were transferred into a 1.5-mL micro-centrifuge tube containing 500  $\mu\text{L}$  of 100 mM HEPES (pH 7.6) buffer and 400  $\mu\text{L}$  of ultra-pure water. 40  $\mu\text{L}$  of this mixture were taken, mixed with 360  $\mu\text{L}$  of ultrapure water, and added to a LC-MS glass vial containing 600  $\mu\text{L}$  of 100% acetonitrile (control). Second, 10  $\mu\text{L}$  of 1 M  $\text{MgCl}_2$ , 10  $\mu\text{L}$  of 100 mM ATP and 20  $\mu\text{L}$  of 250 U/mL hexokinase prepared in HEPES (pH 7.6) were supplemented to the remaining 960  $\mu\text{L}$  of the sample. Free  $^{13}\text{C}$ -fructose and  $^{13}\text{C}$ -glucose were: (i) phosphorylated for 2 h at  $25^{\circ}$ , (ii) placed in a boiling-water bath for 10 min in order to inactivate hexokinase, and (iii) directly transferred onto ice for 10 min. At this point, a 40  $\mu\text{L}$  aliquot was taken and added to a 1.5 mL microcentrifuge tube containing 360  $\mu\text{L}$  of ultrapure water. The 400  $\mu\text{L}$  of extract was then transferred to a 3kDa Amicon filtering device, and spun at  $14,000\times g$  for 30 min. The eluate was added to a LC-MS glass vial containing 600  $\mu\text{L}$  of 100% acetonitrile. Third, 40  $\mu\text{L}$  of 1250 U/mL invertase were added to the sample followed by a 2 h incubation at  $25\text{ }^{\circ}\text{C}$ . After invertase treatment, a 400  $\mu\text{L}$  aliquot was taken, loaded onto a 3 kDa Amicon filtering device, and centrifuged at  $14,000\times g$  for 30 min. Finally, the flow through was transferred into a LC-MS/MS glass vials containing 600  $\mu\text{L}$  of 100% acetonitrile. The mass isotopomer distribution of free  $^{13}\text{C}$ -glucose, free  $^{13}\text{C}$ -fructose,  $^{13}\text{C}$ -glucosyl and  $^{13}\text{C}$ -fructosyl moieties generated from  $^{13}\text{C}$ -sucrose cleavage were analyzed by LC-MS/MS using multiple reaction monitoring mode. The LC and MS conditions were the same as those of previous work [24].

**Supplementary Materials:** The following are available online at <http://www.mdpi.com/2218-1989/10/1/30/s1>, Table S1:  $^{13}\text{C}$  mass isotopomer abundances of glucose and fructose, Table S2:  $^{13}\text{C}$  mass isotopomer abundances of fructosyl and glucosyl moieties after sucrose cleavage.

**Author Contributions:** Conceptualization, J.-C.C. and A.P.A. Methodology, J.-C.C. and A.P.A. Validation, J.-C.C. and Z.R. Formal Analysis, J.-C.C. and Z.R. Investigation, J.-C.C. and A.P.A. Resources, A.P.A. Data Curation, J.-C.C. and Z.R. Writing—Original Draft Preparation, J.-C.C. and A.P.A. Writing—Review & Editing, J.-C.C., Z.R. and A.P.A. Visualization, J.-C.C., Z.R. and A.P.A. Supervision, J.-C.C. and A.P.A. Project Administration, A.P.A. Funding Acquisition, A.P.A. All authors have read and agreed to the published version of the manuscript.

**Funding:** This material is based upon work partially supported by the Agriculture and Food Research Initiative competitive grant # 2016-67013-29020 from the USDA National Institute of Food and Agriculture, and by the U.S. Department of Energy, Office of Science, Office of Biological and Environmental Research (BER), grant # DE-SC0019233 to A.P.A., and Genomic Science Program grant # DE-SC0020325 to A.P.A.

**Conflicts of Interest:** The authors declare no conflict of interest.

## References

1. Ratcliffe, R.G.; Shachar-Hill, Y. Measuring multiple fluxes through plant metabolic networks. *Plant J.* **2006**, *45*, 490–511. [[CrossRef](#)] [[PubMed](#)]
2. Hatzfeld, W.D.; Stitt, M. A study of the rate of recycling of triose phosphates in heterotrophic *Chenopodium rubrum* cells, potato tubers, and maize endosperm. *Planta* **1990**, *180*, 198–204. [[CrossRef](#)] [[PubMed](#)]
3. Hill, S.A.; ap Rees, T. Fluxes of carbohydrate metabolism in ripening bananas. *Planta* **1993**, *192*, 52–60. [[CrossRef](#)]
4. Salon, C.; Raymond, P.; Pradet, A. Quantification of carbon fluxes through the tricarboxylic acid cycle in early germinating lettuce embryos. *J. Biol. Chem.* **1988**, *263*, 12278–12287. [[PubMed](#)]

5. Bowsher, C.G.; Tobin, A.K. Compartmentation of metabolism within mitochondria and plastids. *J. Exp. Bot.* **2001**, *52*, 513–527. [[CrossRef](#)] [[PubMed](#)]
6. Lunn, J.E. Compartmentation in plant metabolism. *J. Exp. Bot.* **2007**, *58*, 35–47. [[CrossRef](#)]
7. Dieuaide-Noubhani, M.; Alonso, A.P. Application of metabolic flux analysis to plants. *Methods Mol. Biol.* **2014**, *1090*, 1–18.
8. Alonso, A.P.; Piasecki, R.J.; Wang, Y.; LaClair, R.W.; Shachar-Hill, Y. Quantifying the Labeling and the Levels of Plant Cell Wall Precursors Using Ion Chromatography Tandem Mass Spectrometry. *Plant Physiol.* **2010**, *153*, 915–924. [[CrossRef](#)]
9. Cocuron, J.C.; Alonso, A.P. Liquid chromatography tandem mass spectrometry for measuring <sup>13</sup>C-labeling in intermediaries of the glycolysis and pentose-phosphate pathway. *Methods Mol. Biol.* **2014**, *1090*, 131–142.
10. Allen, D.K.; Shachar-Hill, Y.; Ohlrogge, J.B. Compartment-specific labeling information in C-13 metabolic flux analysis of plants. *Phytochemistry* **2007**, *68*, 2197–2210. [[CrossRef](#)]
11. Alonso, A.P.; Dale, V.L.; Shachar-Hill, Y. Understanding fatty acid synthesis in developing maize embryos using metabolic flux analysis. *Metab. Eng.* **2010**, *12*, 488–497. [[CrossRef](#)]
12. Alonso, A.P.; Goffman, F.D.; Ohlrogge, J.B.; Shachar-Hill, Y. Carbon conversion efficiency and central metabolic fluxes in developing sunflower (*Helianthus annuus* L.) embryos. *Plant J.* **2007**, *52*, 296–308. [[CrossRef](#)] [[PubMed](#)]
13. Alonso, A.P.; Raymond, P.; Hernould, M.; Rondeau-Mouro, C.; de Graaf, A.; Chourey, P.; Lahaye, M.; Shachar-Hill, Y.; Rolin, D.; Dieuaide-Noubhani, M. A metabolic flux analysis to study the role of sucrose synthase in the regulation of the carbon partitioning in central metabolism in maize root tips. *Metab. Eng.* **2007**, *9*, 419–432. [[CrossRef](#)] [[PubMed](#)]
14. Alonso, A.P.; Raymond, P.; Rolin, D.; Dieuaide-Noubhani, M. Substrate cycles in the central metabolism of maize root tips under hypoxia. *Phytochemistry* **2007**, *68*, 2222–2231. [[CrossRef](#)] [[PubMed](#)]
15. Alonso, A.P.; Val, D.L.; Shachar-Hill, Y. Central metabolic fluxes in the endosperm of developing maize seeds and their implications for metabolic engineering. *Metab. Eng.* **2011**, *13*, 96–107. [[CrossRef](#)]
16. Cocuron, J.C.; Koubaa, M.; Kimmelfield, R.; Ross, Z.; Alonso, A.P. A combined metabolomics and fluxomics analysis identifies steps limiting synthesis in maize embryos. *Plant Physiol.* **2019**, *181*, 961–975. [[CrossRef](#)]
17. Dieuaidenoubhani, M.; Raffard, G.; Canioni, P.; Pradet, A.; Raymond, P. Quantification of Compartmented Metabolic Fluxes in Maize Root-Tips Using Isotope Distribution from C-13-Labeled or C-14-Labeled Glucose. *J. Biol. Chem.* **1995**, *270*, 13147–13159. [[CrossRef](#)]
18. Masakapalli, S.K.; Le Lay, P.; Huddleston, J.E.; Pollock, N.L.; Kruger, N.J.; Ratcliffe, R.G. Subcellular Flux Analysis of Central Metabolism in a Heterotrophic Arabidopsis Cell Suspension Using Steady-State Stable Isotope Labeling. *Plant Physiol.* **2010**, *152*, 602–619. [[CrossRef](#)]
19. Rontein, D.; Dieuaide-Noubhani, M.; Dufourc, E.J.; Raymond, P.; Rolin, D. The metabolic architecture of plant cells - Stability of central metabolism and flexibility of anabolic pathways during the growth cycle of tomato cells. *J. Biol. Chem.* **2002**, *277*, 43948–43960. [[CrossRef](#)]
20. Alonso, A.P.; Vigeolas, H.; Raymond, P.; Rolin, D.; Dieuaide-Noubhani, M. A new substrate cycle in plants. evidence for a high glucose-phosphate-to-glucose turnover from in vivo steady-state and pulse-labeling experiments with [<sup>13</sup>C] glucose and [<sup>14</sup>C] glucose. *Plant Physiol.* **2005**, *138*, 2220–2232. [[CrossRef](#)]
21. Fell, D. *Understanding the Control of Metabolism*; Portland Press: London, UK, 1997; pp. 213–225.
22. Acket, S.; Degournay, A.; Merlier, F.; Thomasset, B. <sup>13</sup>C labeling analysis of sugars by high resolution-mass spectrometry for metabolic flux analysis. *Anal. Biochem.* **2017**, *527*, 45–48. [[CrossRef](#)] [[PubMed](#)]
23. Viola, R.; Davies, H.V.; Chudeck, A.R. Pathways of starch and sucrose biosynthesis in developing tubers of potato (*Solanum tuberosum* L.) and seeds of faba bean (*Vicia faba* L.): Elucidation by <sup>13</sup>C-nuclear-magnetic-resonance spectroscopy. *Planta* **1991**, *183*, 202–208. [[CrossRef](#)] [[PubMed](#)]
24. Cocuron, J.C.; Anderson, B.; Boyd, A.; Alonso, A.P. Targeted metabolomics of *Physaria fendleri*, an industrial crop producing hydroxy fatty acids. *Plant Cell Physiol.* **2014**, *55*, 620–633. [[CrossRef](#)]
25. Calvano, C.D.; Cataldi, T.R.I.; Kogel, J.F.; Monopoli, A.; Palmisano, F.; Sundermeyer, J. Structural Characterization of Neutral Saccharides by Negative Ion MALDI Mass Spectrometry Using a Superbasic Proton Sponge as Deprotonating Matrix. *J. Am. Soc. Mass Spectrom.* **2017**, *28*, 1666–1675. [[CrossRef](#)] [[PubMed](#)]

26. Koubaa, M.; Cocuron, J.-C.; Thomasset, B.; Alonso, A.P. Highlighting the tricarboxylic acid cycle: Liquid and gas chromatography-mass spectrometry analyses of  $^{13}\text{C}$ -labeled organic acids. *Anal. Biochem.* **2013**, *436*, 151–159. [[CrossRef](#)] [[PubMed](#)]
27. Cocuron, J.C.; Tsogtbaatar, E.; Alonso, A.P. High-throughput quantification of the levels and labeling abundance of free amino acids by liquid chromatography tandem mass spectrometry. *J. Chromatogr. A* **2017**, *1490*, 148–155. [[CrossRef](#)] [[PubMed](#)]



© 2020 by the authors. Licensee MDPI, Basel, Switzerland. This article is an open access article distributed under the terms and conditions of the Creative Commons Attribution (CC BY) license (<http://creativecommons.org/licenses/by/4.0/>).